

FAR ULTRAVIOLET SPECTROSCOPIC EXPLORER OBSERVATIONS OF INTERSTELLAR GAS TOWARD THE LARGE MAGELLANIC CLOUD STAR Sk −67°05

S. D. FRIEDMAN,¹ J. C. HOWK,¹ B-G ANDERSSON,¹ K. R. SEMBACH,¹ T. B. AKE,¹ K. ROTH,¹ D. J. SAHNEW,¹
 B. D. SAVAGE,² D. G. YORK,³ G. SONNEBORN,⁴ A. VIDAL-MADJAR,⁵ AND E. WILKINSON⁶

Received 2000 March 24; accepted 2000 June 8; published 2000 July 19

ABSTRACT

We report on measurements of interstellar O VI, H₂, P II, Si II, Ar I, and Fe II absorption along the line of sight to Sk −67°05, a B0 Ia star in a diffuse H II region in the western edge of the Large Magellanic Cloud (LMC). We find $\log N(\text{O VI}) = 14.40 \pm 0.04$ in the Milky Way component and, using the C IV column density from previous *IUE* observations, $N(\text{C IV})/N(\text{O VI}) = 1.00 \pm 0.16$, a value similar to other halo measurements made with the *Far Ultraviolet Spectroscopic Explorer*. In the LMC component, $\log N(\text{O VI}) = 13.89 \pm 0.05$ and $N(\text{C IV})/N(\text{O VI}) < 0.4$ (3 σ), since only an upper limit on $N(\text{C IV})$ is available. Along this sight line, the LMC is rich in molecular hydrogen [$\log N(\text{H}_2) = 19.50 \pm 0.08$]; in the Milky Way, $\log N(\text{H}_2) = 14.95 \pm 0.08$. A two-component fit for the excitation temperature of the molecular gas in the LMC gives $T_{01} = 59 \pm 5$ K for $J = 0$, 1 and $T_{\text{ex}} = 800 \pm 330$ K for $J = 3, 4, 5$. For the Milky Way, $T_{01} = 99^{+30}_{-20}$ K; no excitation temperature could be determined for the higher rotational states. The Milky Way and LMC gas-phase [Fe/P] abundances are ~ 0.6 and ~ 0.7 dex lower, respectively, than solar system abundances. These values are similar to [Fe/Zn] measurements for the Milky Way and LMC toward SN 1987A.

Subject headings: galaxies: individual (Large Magellanic Cloud) — ISM: atoms — ultraviolet: ISM

1. INTRODUCTION

The analysis of interstellar absorption lines provides fundamental information about the content and physical conditions of the interstellar medium (ISM). Absorption-line spectroscopy can be used to study the ISM in our Galaxy, in nearby systems such as the Magellanic Clouds, and in the intergalactic medium out to the most distant QSOs. These studies provide an opportunity to compare elemental abundances and physical conditions in regions with differing chemical histories.

As part of a general program to investigate the interstellar medium of the Milky Way and nearby galaxies, we have used the *Far Ultraviolet Spectroscopic Explorer* (*FUSE*) satellite (Moos et al. 2000) to observe the star Sk −67°05 (HD 268605) in the Large Magellanic Cloud (LMC). The first observations of Galactic halo gas with *IUE* were along sight lines to stars in the LMC (Savage & de Boer 1979, 1981). In this Letter, we discuss the first *FUSE* observations of an LMC star revealing O VI absorption in both the Milky Way and LMC. We also discuss the measurements of H₂, P II, Si II, Ar I, and Fe II absorption along this sight line.

2. OBSERVATIONS AND DATA PROCESSING

Sk −67°05 ($l = 278^\circ 89$, $b = -36^\circ 32$) is a B0 Ia star (Smith Neubig & Bruhweiler 1999) located near the western edge of the LMC. It lies in a diffuse H II region (Chu et al. 1994) with relatively low diffuse X-ray emission compared to regions closer to the center of the LMC (Snowden & Petre 1994). Ardeberg

et al. (1972) give $B - V = -0.12$, and for $(B - V)_0 = -0.23$ (Binney & Merrifield 1998), we find $E(B - V) = 0.11$. Using the Galactic gas-to-dust correlation (Diplas & Savage 1994), we infer $N(\text{H I}) \sim 5.4 \times 10^{20} \text{ cm}^{-2}$ along this sight line.

This star was observed during the in-orbit checkout phase of the mission (Sahnew et al. 2000) at various times between 1999 August 20 and October 19. As these observations were part of tests designed primarily to align the four optical channels in the instrument, the star was stepped across the $30'' \times 30''$ aperture during the observations. However, the data were taken in time-tagged photon-address mode, so that corrections could be made for this image motion. The analysis here uses LiF1 (990–1080 Å) data only; the LiF2 channel has lower sensitivity and poorer flat-field characteristics, and during this period no flat-field corrections were available. The SiC (905–1100 Å) channels were generally not aligned. The instrument was still in its preflight focus configuration, and the spectral resolution was $\lambda/\Delta\lambda \approx 15,000$. The wavelength scale was established with a preflight dispersion solution. However, because of the stepping manner in which the data were obtained, additional zero-point adjustments were required. Relative velocities are generally accurate to $\sim 10 \text{ km s}^{-1}$ over limited spectral ranges, and the absolute scale was set by comparison with *IUE* spectra. The data presented represent a total of approximately 33 ks of on-target exposure time for the LiF1A and 35 ks for the LiF1B spectral regions, approximately equally split between day and night. Additional details of the data processing for this data set can be found elsewhere (Massa et al. 2000).

This star exhibits variable stellar wind features. However, as shown in Figure 3 of Massa et al. (2000), the variability is minimal at the wavelengths of interest here and does not affect our conclusions.

3. INTERSTELLAR ABSORPTION FEATURES

Figure 1 shows the composite spectrum from the LiF1 channel. Several metal lines that appear in the ISM of both the Milky Way and LMC are identified. Most other lines are due

¹ Department of Physics and Astronomy, Johns Hopkins University, Baltimore, MD 21218.

² Department of Astronomy, University of Wisconsin, Madison, WI 53706.

³ Department of Astronomy and Astrophysics, University of Chicago, Chicago, IL 60637.

⁴ Laboratory for Astronomy and Solar Physics, NASA Goddard Space Flight Center, Code 681, Greenbelt, MD 20771.

⁵ Institut d'Astrophysique de Paris, Centre National de la Recherche Scientifique, 98 bis Boulevard Arago, F-75014 Paris, France.

⁶ Center for Astrophysics and Space Astronomy, University of Colorado, Campus Box 389, Boulder, CO 80309.

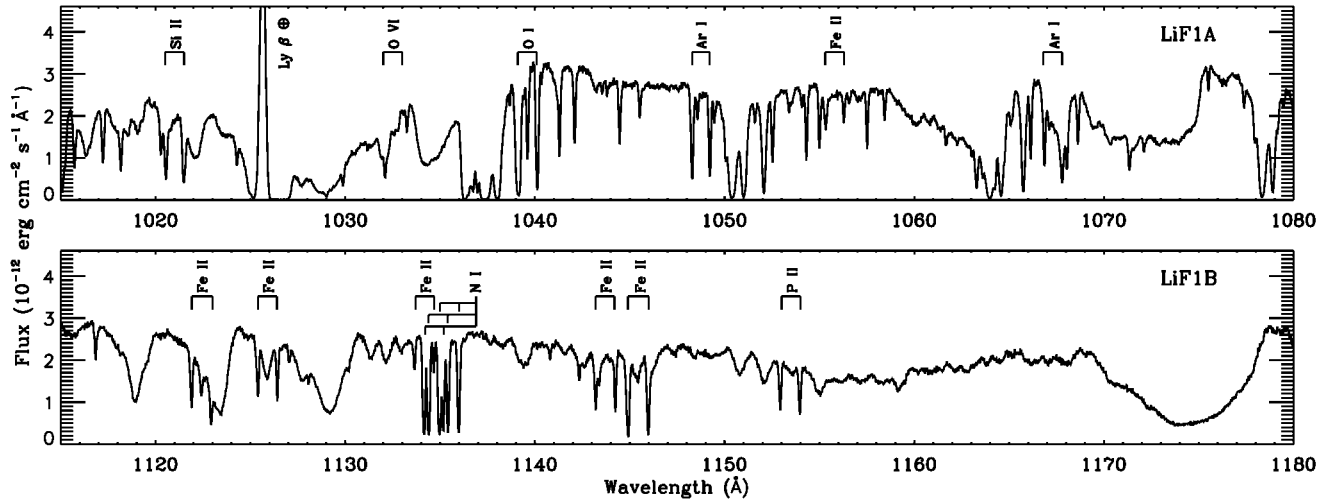


FIG. 1.—Composite LiF1A and LiF1B spectra of Sk $-67^{\circ}05$. Several important metal lines having components in both the Milky Way and LMC are marked. Most of the other absorption lines are due to molecular hydrogen in the LMC. The strong emission line at 1025.72 Å is due to terrestrial Ly β airglow. The fully sampled data has been smoothed by 4 pixels in these plots. This smoothing does not affect the observed line widths because the data are oversampled.

to H₂ absorption in the LMC. The strong emission line is terrestrial Ly β λ 1025.72 airglow from the daytime exposures.

In this analysis, we have used only the λ 1031.93 member of the O VI doublet since the λ 1037.62 line is blended with C IV λ 1037.02 and several H₂ lines. Figure 2 shows the *FUSE* O VI λ 1031.93 absorption line and a high-dispersion *IUE* spectrum of C IV λ 1550.77. The H₂ (6–0) *P*(3) line originating in the LMC appears at +88 km s^{−1} and must be modeled and removed to get an accurate estimate of the O VI column density.

We have analyzed the (2–0) to (9–0) H₂ Lyman bands, using the method described in Shull et al. (2000) to determine the equivalent widths, *b*-values, and column densities for the Milky Way and LMC components of H₂. Since the typical spacing between the rotational-vibrational lines within each Lyman band is very close to the spacing between LMC and the Milky

Way absorption, the measurement of the Milky Way H₂ depends on a careful decomposition of blended lines. Because of this difficulty, we used only the (4–0) and (2–0) Lyman bands to measure the *J* = 0, 1 levels from the Milky Way gas.

The results of the H₂ model, discussed below, give log *N*(H₂) = 15.28 for the (6–0) *P*(3) line in the LMC. This was convolved with the instrumental resolution of 25 km s^{−1} and divided out of the original spectrum to remove the effects of the H₂ absorption. The resulting O VI profile is shown as a light line in Figure 2.

To calculate the O VI absorption, we have considered two possible continuum placements, designated “high” and “low,” which are displayed in Figure 2 as long-dashed and dash-dotted lines, respectively. The arrow at +180 km s^{−1} denotes the velocity we have adopted as separating the Milky Way and LMC components of O VI. Table 1 gives O VI equivalent widths derived using both continua.

Figure 3 shows the spectra of several important metal lines

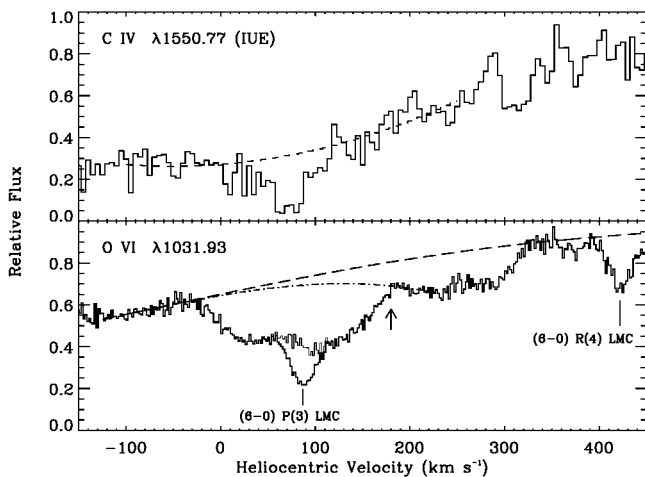


FIG. 2.—O VI λ 1031.93 line profile from *FUSE* and the C IV λ 1550.77 line profile from *IUE*. The velocity scale has been adjusted as described in the text. Both “high” (long-dashed line) and “low” (dash-dotted line) continuum placements have been considered in the O VI analysis. The arrow denotes the adopted division between the Milky Way gas at velocities less than 180 km s^{−1} and the LMC gas at velocities greater than 180 km s^{−1}. The H₂ (6–0) *P*(3) line, arising in the LMC, falls directly in the Milky Way O VI absorption line. The model fit has been divided out to remove the effects of the H₂ absorption, and the resulting O VI profile is shown as a light line.

TABLE 1
IONIC EQUIVALENT WIDTHS

ION	λ	$\log \lambda^f$	W_λ (mÅ) ^a	
			Milky Way	LMC
O VI	1031.926	2.14	249 ± 10 ^b	87 ± 5 ^b
	1031.926	2.14	213 ± 8 ^c	...
Si II	1020.699	1.46	99 ± 3	143.0 ± 2.4
P II	1152.818	2.43	74.3 ± 2.1	78.6 ± 1.7
Ar I	1048.220	2.41	127.0 ± 2.2	105.2 ± 2.4
Fe II	1055.262	0.81	...	31.0 ± 1.9
	1112.048	0.84 ^d	...	34.5 ± 1.9
	1121.975	1.35 ^d	85.4 ± 1.9	81 ± 3
	1125.448	1.24	77.8 ± 2.3	66.7 ± 2.3
	1127.098	0.48 ^d	16.2 ± 1.9	11.2 ± 1.1
	1133.665	0.74	38 ± 5	...
	1142.366	0.63	16 ± 3	...
	1144.938	2.10	173 ± 4	...

^a Measured equivalent widths and 1 σ uncertainties (in mÅ) for the Milky Way and LMC components toward Sk $-67^{\circ}05$.

^b Derived using the “high” continuum (see text).

^c Derived using the “low” continuum (see text). Probable contamination from H₂ (6–0) *P*(3) 1031.19 Å line removed.

^d Oscillator strength taken from the preliminary results of Howk et al. 2000.

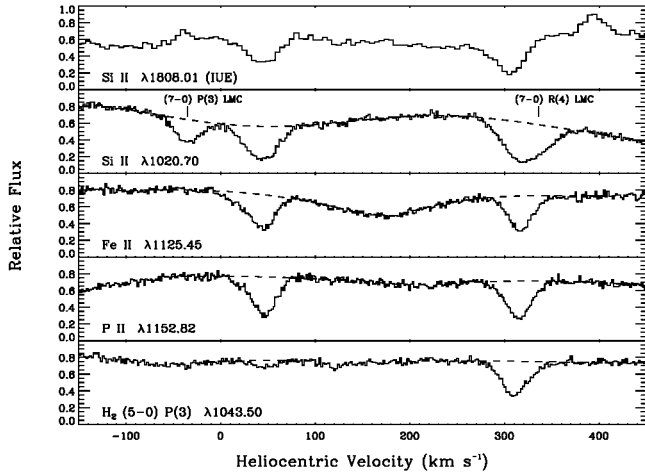


FIG. 3.—Selected absorption lines of low ions in the *FUSE* bandpass, together with the Si II $\lambda 1808.01$ line from *IUE* observations. Dashed lines show the adopted continuum levels. The equivalent widths of the Milky Way and LMC components are given in Table 1. The velocity scales of the *FUSE* lines have been adjusted to make the Milky Way component velocities match those of the Si II *IUE* line. The LMC component of Si II $\lambda 1020.70$ is broadened due to a blend with the indicated H_2 line.

and a molecular hydrogen line along the sight line to Sk $-67^\circ 05$. For comparison, the *IUE* spectrum of Si II $\lambda 1808.01$ is shown. The individual absorption lines have separately been shifted in velocity to align the Milky Way components with the corresponding feature in the *IUE* spectrum. We established the velocity scale for the O VI region by shifting the Si II $\lambda 1020.70$ line to match the Si II $\lambda 1808.01$ *IUE* velocity scale, which sets the velocities of the nearby H_2 Lyman (7–0) $P(2)$ $\lambda 1016.46$ and $P(3)$ $\lambda 1019.50$ lines. The (6–0) $P(3)$ $\lambda 1031.19$ and $R(4)$ $\lambda 1032.35$ lines were then used to establish the O VI velocity, as shown in Figure 2. The measured equivalent widths of several interstellar metal lines are also given in Table 1.

The adopted column densities for several ionic species, as well as several rotational states of H_2 along this sight line, are given in Table 2. These were calculated by fitting to a single-component Doppler-broadened curve of growth for Fe II and H_2 and by using the apparent column density method (Savage & Sembach 1991) for the other species listed. The two values given for the O VI column are based on the high and low continuum placements. We have added a systematic error of 0.04 dex in quadrature with the statistical error for O VI to account for errors in continuum placement and the velocity interval over which the apparent column density is integrated.

4. DISCUSSION

Since 114 eV are required to convert O^{+4} to O^{+5} , O VI is almost never produced by photoionization from starlight. Thus, it is a sensitive tracer of hot ($\sim 300,000$ K) collisionally ionized gas in the interstellar medium. Adopting the high continuum placement shown in Figure 2, which we believe is more appropriate, the O VI column density is $\log N(O\text{ VI}) = 14.40 \pm 0.02$ and 13.89 ± 0.03 in the Milky Way and LMC, respectively. For the Milky Way gas, $\log [N(O\text{ VI}) \sin |b|] = 14.17$, which agrees well with the median value of 14.21 along 11 Galactic halo sight lines studied by Savage et al. (2000).

Using $\log N(C\text{ IV}) = 14.41$ in the Milky Way from Wakker et al. (1998) and assuming an error of 0.05 dex, we find $N(C\text{ IV})/N(O\text{ VI}) = 1.00 \pm 0.16$. If the low continuum is

TABLE 2
ADOPTED COLUMN DENSITIES

SPECIES	$\log N\text{ (cm}^{-2}\text{)}^a$		METHOD ^b
	Milky Way	LMC	
O VI	14.40 ± 0.02^c	13.89 ± 0.03^c	1
O VI	14.32 ± 0.02^d	...	1
P II	≥ 13.5	≥ 13.6	1
Si II	≥ 13.9	≥ 14.5	1
Ar I	≥ 14.0	≥ 13.8	1
Fe II	14.8 ± 0.1	14.8 ± 0.1	2
H_2 ($J = 0$)	14.26 ± 0.09	19.34 ± 0.10	2
H_2 ($J = 1$)	14.46 ± 0.08	18.99 ± 0.10	2
H_2 ($J = 2$)	$14.41^{+0.15}_{-0.21}$	$16.28^{+0.30}_{-0.50}$	2
H_2 ($J = 3$)	$14.23^{+0.13}_{-0.19}$	$15.28^{+0.30}_{-0.50}$	2
H_2 ($J = 4$)	14.46 ± 0.06	2
H_2 ($J = 5$)	$14.62^{+0.18}_{-0.30}$	2

^a Logarithm of the adopted column densities for the Milky Way and LMC components toward Sk $-67^\circ 05$ (in units of ions cm^{-2}).

^b Method used for deriving column densities: (1) apparent column density method; (2) curve-of-growth fitting method.

^c Column density using “high” continuum (see text).

^d Column density using “low” continuum (see text).

adopted, this ratio is 1.23 ± 0.20 . Either value is greater than, but consistent with, the halo value $\langle N(C\text{ IV})/N(O\text{ VI}) \rangle \sim 0.6$ determined from *FUSE* observations of four extragalactic sight lines (Savage et al. 2000), as well as $\langle N(C\text{ IV})/N(O\text{ VI}) \rangle \sim 0.9$ from *Copernicus* and *IUE* observations of stars in the lower halo (Spitzer 1996).

Note that the widths of O VI components in both the Milky Way and LMC are much broader than the thermal line width, which is $\approx 30\text{ km s}^{-1}$ (FWHM) for gas at 300,000 K. The substantial difference in the widths of the C IV and O VI lines may be due to the different scale heights in the Galactic halo of these ions (Savage et al. 2000).

Sk $-67^\circ 05$ was the only star for which Wakker et al. (1998) did not detect C IV in their study of the LMC halo. We recalculated their upper limit to $N(C\text{ IV})$ assuming the velocity range observed in the O VI gas ($+180$ to $+322\text{ km s}^{-1}$) and find $\log N(C\text{ IV}) < 13.5$ (3σ). Adopting the high continuum case, we find $N(C\text{ IV})/N(O\text{ VI}) < 0.4$ (3σ) for the LMC material along the Sk $-67^\circ 05$ sight line.

The H_2 column density varies greatly between the LMC and Milky Way. For the LMC, we find $\log N(H_2) = 19.50 \pm 0.08$, summed over the $J = 0-5$ states (Table 2), and a b -value of $5 \pm 2\text{ km s}^{-1}$. This column density is significantly higher than that measured along other LMC sight lines (de Boer et al. 1998; Shull et al. 2000). By comparison, *FUSE* observations of the metal-deficient galaxy I Zw 18 have yielded only an upper limit, $\log N(H_2) \lesssim 15$ (Vidal-Madjar et al. 2000).

The distribution of H_2 rotational states in the LMC is best fitted by a two-component excitation temperature (Fig. 4) with $T_{01} = 59 \pm 5\text{ K}$ for $J = 0, 1$ and $T_{\text{ex}} = 800 \pm 330\text{ K}$ for $J = 3, 4, 5$. This is similar to the temperature distribution seen along the sight line to star LH 10:3120 in the LMC using *ORFEUS* (de Boer et al. 1998). This indicates that the gas is not in thermal equilibrium and the higher J states are fluorescently pumped by UV radiation. This excited gas may therefore exist in the outer, optically thin regions of the cloud. In the interior regions the molecular fraction may increase due to self-shielding, which is expected when $E(B-V) \gtrsim 0.1$ (Savage et al. 1977). The $J = 2$ point falls almost exactly on the extension of the T_{01} line, suggesting that the density of this gas is rather high.

For the Milky Way gas, we find an H_2 column density of $\log N(H_2) = 14.95 \pm 0.08$, summed over the $J = 0-3$ states (Table 2), and a rotational temperature of $T_{01} = 99^{+30}_{-20}\text{ K}$

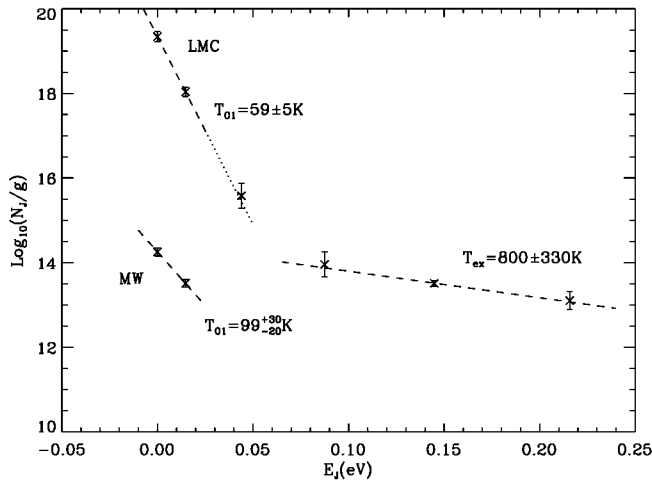


FIG. 4.—Column densities for the $J = 0-5$ levels of H_2 in the LMC and Milky Way. For the LMC a two-component fit is possible, with the excitation temperatures indicated. For the much weaker Milky Way lines, reliable column densities could only be determined for the $J = 0$ and 1 levels. Note that the dotted line extension of the LMC T_{01} line intersects the $J = 2$ point, indicating that the density of this gas is rather high. The LMC H_2 column densities shown here are significantly higher than those reported along other LMC sight lines (de Boer et al. 1998; Shull et al. 2000).

(Fig. 4). This temperature is similar to other values measured with *FUSE* (Shull et al. 2000) and to *Copernicus* measurements of Galactic stars (Savage et al. 1977). There is an indication of a two-component temperature distribution for the Milky Way gas as well. However, because of the relatively small number of measurable lines and severe blending, we are unable to accurately determine an excitation temperature for the higher J Milky Way material.

Absorption from both Milky Way and LMC material is clearly seen in all of the low ions present in the LiF1 data (e.g., Figs. 1 and 3). Blending of atomic, ionic, and H_2 absorption along this sight line limits the number of species for which we can derive accurate equivalent widths and column densities. The depleted species Fe II has several well-observed transitions in our data set (Table 1). We have constructed a single-component Doppler-broadened curve of growth for the Fe II lines observed in both the Milky Way and the LMC. The best fit yields $\log N(\text{Fe II}) = 14.8 \pm 0.1$ and 14.8 ± 0.1 with $b = 14.2 \pm 0.5$ and $12.1^{+2.1}_{-1.6}$ km s^{-1} for the Milky Way and LMC, respectively. Due to potential uncertainties in some of the f -values, we have adopted a conservative error of 0.1 dex in these column densities. Our data permit good measurements of the nondepleted species P II $\lambda 1152.82$, and we derive lower limits to the Milky Way and LMC column densities (Table 2)

using the apparent column density method. If the b -values for P II are similar to those derived for Fe II, the data suggest only very moderate saturation corrections of $\lesssim 0.1$ dex.

For the sight line through the halo of the Milky Way, we derive a gas-phase abundance $[\text{Fe/P}] \equiv \log N(\text{Fe II}) - \log N(\text{P II}) - \log (\text{Fe/P})_{\odot} \sim -0.6$, assuming a solar system ratio of $\log (\text{Fe/P})_{\odot} = +1.92$ (Anders & Grevesse 1989). For the LMC gas along this direction, we find $[\text{Fe/P}] \sim -0.7$. This suggests significant incorporation of iron into dust grains in both galaxies. Differences in the relative abundance of singly and doubly ionized iron and phosphorous could affect this measurement (Sembach et al. 2000), but the magnitude of this effect is likely to be much too small to account for the gas-phase deficiency of iron along this sight line. The derived values of $[\text{Fe/P}]$ are similar to the values of $[\text{Fe/Zn}] = -1.06$ and -0.91 for the Milky Way halo and LMC absorption toward SN 1987A (Welty et al. 1999). Future *FUSE* observations of a large number of LMC sight lines will allow us to study the distribution of gas-phase abundances and infer the composition of interstellar dust in this environment.

5. SUMMARY

We have reported equivalent widths and column densities of O VI, H_2 , P II, Si II, Ar I, and Fe II along the line of sight to Sk -67°05 in the LMC using *FUSE* data. The principal results of this study are:

1. In the halo of the Milky Way toward the LMC $N(\text{C IV})/N(\text{O VI}) = 1.00 \pm 0.16$, a value somewhat greater than but consistent with other *FUSE* observations through the halo (Savage et al. 2000). In the LMC, where only an upper limit on $N(\text{C IV})$ is available, we find $N(\text{C IV})/N(\text{O VI}) < 0.4$ (3σ). This is consistent with the lower ratio seen in the disk of the Milky Way compared to the halo (Savage et al. 2000; Spitzer 1996).
2. The LMC is rich in H_2 along this sight line, $\log N(H_2) = 19.50 \pm 0.08$. A two-component temperature fit gives $T_{01} = 59 \pm 5$ K for and $T_{\text{ex}} = 800 \pm 330$ K.
3. The gas-phase abundances of $[\text{Fe/P}] \sim -0.6$ and ~ -0.7 in the Milky Way and LMC suggest significant depletion in both locations relative to solar abundances.

We thank D. Massa for providing the software to co-add the spectra used in this analysis. This work is based on data obtained for the Guaranteed Time Team by the NASA-CNES-CSA *FUSE* mission operated by Johns Hopkins University. Financial support to US participants has been provided by NASA contract NAS5-32985.

REFERENCES

- Anders, E., & Grevesse, N. 1989, *Geochim. Cosmochim. Acta*, 53, 197
 Ardeberg, A., Brunet, J. P., Maurice, E., & Prevot, L. 1972, *A&AS*, 6, 249
 Binney, J., & Merrifield, M. 1998, *Galactic Astronomy* (Princeton: Princeton Univ. Press)
 Chu, Y.-H., Wakker, B., Mac Low, M. M., & Garcia-Segura, G. 1994, *AJ*, 108, 1696
 de Boer, K. S., Richter, P., Bomans, D. J., Heithausen, A., & Koorneef, J. 1998, *A&A*, 338, L5
 Diplas, A., & Savage, B. D. 1994, *ApJ*, 427, 274
 Howk, J. C., Sembach, K. R., Roth, K. C., & Kruk, J. W. 2000, *ApJ*, submitted
 Massa, D., et al. 2000, *ApJ*, 538, L47
 Moos, H. W., et al. 2000, *ApJ*, 538, L1
 Sahnou, D. J., et al. 2000, *ApJ*, 538, L7
 Savage, B. D., Bohlin, R. C., Drake, J. F., & Budich, W. 1977, *ApJ*, 216, 291
 Savage, B. D., & de Boer, K. S. 1979, *ApJ*, 230, L77
 Savage, B. D., & de Boer, K. S. 1981, *ApJ*, 243, 460
 Savage, B. D., & Sembach, K. R. 1991, *ApJ*, 379, 245
 Savage, B. D., et al. 2000, *ApJ*, 538, L27
 Sembach, K. R., Howk, J. C., Ryans, R. S., & Keenan, F. P. 2000, *ApJ*, 528, 310
 Shull, J. M., et al. 2000, *ApJ*, 538, L73
 Smith Neubig, M. M., & Bruhweiler, F. C. 1999, *AJ*, 117, 2856
 Snowden, S. L., & Petre, R. 1994, *ApJ*, 436, L123
 Spitzer, L. 1996, *ApJ*, 458, L29
 Vidal-Madjar, A., et al. 2000, *ApJ*, 538, L77
 Wakker, B. P., Howk, J. C., Chu, Y.-H., Bomans, D., & Points, S. D. 1998, *ApJ*, 499, L87
 Welty, D. E., Frisch, P. C., Sonneborn, G., & York, D. G. 1999, *ApJ*, 512, 636